



Adsorptive removal of Cu^{2+} from aqueous solution using aerobic granular sludge

Meipeng Jian, Chaochun Tang*, Ming Liu

School of Civil Engineering and Architecture, East China JiaoTong University, Nanchang 330013, Jiangxi, P.R. China,
Tel./Fax: +86 791 87046027; email: tangcc1964@163.com

Received 24 November 2013; Accepted 1 February 2014

ABSTRACT

Aerobic granular sludge was prepared as adsorbent to remove Cu^{2+} from aqueous solution. Different initial pH values, initial Cu^{2+} concentrations, adsorbent doses, and temperatures on Cu^{2+} adsorption were evaluated. Three kinds of adsorption isotherms (Langmuir model, Freundlich model, and Redlich–Peterson model) were investigated; the results indicated that equilibrium was well described by Langmuir isotherm, predicting the adsorption of Cu^{2+} on aerobic granules was a monolayer adsorption. The equilibrium kinetic adsorption data were fitted to the pseudo-second-order kinetic equation. Furthermore, the sorption of Cu^{2+} was controlled primarily by intraparticle diffusion combined with the kinetics process with Energy-dispersive X-ray spectroscopy (EDS) analysis. Parameters of adsorption thermodynamic suggested that the interaction of Cu^{2+} adsorbed by aerobic granules was spontaneous and exothermic. Moreover, the Fourier transform infrared spectroscopy (FTIR) results indicated that such active groups $-\text{OH}$, $-\text{COOH}$, and $-\text{NH}_2$ were involved in Cu^{2+} adsorption. EDS and FTIR revealed that ion-exchange and surface complexation mechanism coexisted during the adsorption process. Zeta potential analysis demonstrated inner-sphere adsorption happened for Cu^{2+} adsorption on aerobic granules.

Keywords: Aerobic granular sludge; Adsorption; Zeta potential; Mechanisms

1. Introduction

Along with the development of the industrialization, the toxic heavy metal contaminants in wastewater have been becoming more and more serious, and they have already seriously threatened the environment and health security [1]. Various physical–chemical processes have been extensively used in treatment of heavy metal wastewater, which includes chemical precipitation, ion-exchange, electrochemical treatment, etc. However, these conventional techniques have their inherent

limitations such as low efficiency, sensitive operating conditions, product of secondary sludge, and high cost of further disposal [2,3].

Biosorption has been defined as the property of certain biomolecules to bind and concentrate selected ions or other molecules from aqueous solutions. There are many chemical active sites (functional groups) on the surface of biomass, which are responsible for sequestering metals from the surrounding solution [4]. Lately, the biosorption has attracted the attention as a cost-effective and efficient alternative for the removal of heavy metals from wastewaters [5,6]. During recent years, various

*Corresponding author.

naturally available adsorbents like wool, olive cake, sawdust, pine needles, almond shells, cactus leaves, soot, hazelnut shell, coconut shell charcoal, banana peel, seaweed, dead fungal biomass, bacteria, and green alga were used for the removal of heavy metals [7–11]. Thus, it can be seen that the biosorption technology has wide application prospect.

Aerobic granular sludge as the aggregate of self-immobilized bacteria is found to be good biosorbent because of its porous structure and excellent settling properties. In addition, the content of extracellular polymeric substances (EPSs) in aerobic granular sludge is considerably higher than activated sludge, and EPS exhibits a greater ability to complex heavy metals [12–14].

Some previous studies have investigated the influence of many environmental factors on the metal biosorption process. However, there are a limited number of reports on the mechanism of aerobic granules in the removal of Cu^{2+} from aqueous solution. In addition to experiments, a handful of simulation comprehensive studies have been reported on the adsorption of Cu^{2+} in aerobic granular sludge by means of scanning electron microscope (SEM), energy-dispersive X-ray spectroscopy (EDS), Fourier Transform infrared spectroscopy (FTIR), and zeta potential analysis. It is significant to investigate the influence factors and the biosorption mechanism in order to optimize the sorption performance. This work investigated the effect of pH, initial Cu^{2+} concentration, temperature, and biosorbent mass on the adsorption of Cu^{2+} . The isotherms, kinetics, and thermodynamic parameters were explored. The mechanisms of ion-exchange and surface/inner-sphere complexation played in the biosorption were also evaluated.

2. Materials and methods

2.1. Biosorbent

Aerobic granular sludge used for adsorption tests was collected from a laboratory-scale sequencing batch reactor. Aerobic granular sludge was gently washed three times using de-ionized water to remove the surface soluble ions, then dried at 60°C until constant weight was obtained, and finally stored in a desiccator.

2.2. Sorbate

Copper stock solution of $1,000\text{ mg L}^{-1}$ was prepared using $\text{CuSO}_4 \cdot 5\text{H}_2\text{O}$ of analytical reagent

grade into de-ionized water. In this study, the initial Cu^{2+} concentration was varied from 5 to 150 mg L^{-1} .

2.3. Experimental process

2.3.1. Effect of pH

The batch adsorption studies were carried out at different pH values in the range of 1–6. The pH was adjusted using 0.1N NaOH and HCl solutions. 0.1 g aerobic granules were added to 100 mL solution while being shaken at 200 rpm using 250 mL shaking flasks for 12 h in each test.

2.3.2. Effect of contact time and initial Cu^{2+} concentrations

0.1 g of aerobic granular sludge was mixed with 100 mL of various initial Cu^{2+} solutions (30, 50, 100, and 150 mg L^{-1}) in 250 mL shaking flasks at pH 4.77 (optimum value by preliminary test), and suspensions were shaken in a shaker at 200 rpm and 25°C for 12 h.

2.3.3. Effect of biosorbent mass

The effect of biosorbent mass on the amount of Cu^{2+} adsorbed was obtained by agitating 100 mL of Cu^{2+} solution of initial Cu^{2+} concentration of 100 mg L^{-1} with weighed amount of aerobic granules (0.01, 0.02, 0.03, 0.05, 0.08, and 0.1 g) till equilibrium reached at 25°C and at 200 rpm.

2.3.4. Biosorption equilibrium

Equilibrium experiments were performed by contacting 0.1 g of aerobic granules with 100 mL of Cu^{2+} solution of different initial Cu^{2+} concentrations ranging from 5 to 150 mg L^{-1} , which were maintained on an incubated rotary shaker at different temperatures (25 , 35 , and 45°C).

2.3.5. Analysis methods

The specific surface area and pore size were measured on a Micromeritics gas adsorption analyzer instrument (ASAP2020HD88, Micromeritics, USA) equipped with commercial software for calculation and analysis. The surface morphologies and elemental compositions of aerobic granular sludge before and after Cu^{2+} adsorption were examined by SEM (SU-8020, Hitachi, Japan) coupled with EDS (Oxford INCA X, Japan). The pH measurements were made using a pH meter (PHS-3E, China). The zeta potential

of aerobic granule sludge was measured before and after the adsorption of metal ions using zeta-potential analyzer (90Plus, Brookhaven Instruments Corporation, USA); all the Zeta potential values were measured three times and average values were reported. After the experiments, the supernatants were taken from each flask and filtered utilizing a 0.45 μm Millipore filter, and then metal ion concentrations were measured by atomic absorption spectrophotometer (AA-6300C, Oxford, Japan). FTIR spectra of aerobic granular sludge were recorded using FTIR (Spectrum one, Perkin Elmer, USA) connected with a personal computer. FTIR spectra were measured on KBr pellets prepared by pressing mixtures of 1 mg dry powdered sample and 100 mg spectrometry grade KBr under a vacuum to avoid moisture uptake.

3. Results and discussion

3.1. Characterization of aerobic granular sludge

The N_2 sorption properties of the sample were investigated, the BET surface area of aerobic granules was about $2.969 \text{ m}^2 \text{ g}^{-1}$, and the pore size was about 12.723 nm.

SEM/EDS analysis was exploited to illustrate the variation of morphology, mineralogical, and chemical composition for aerobic granular sludge. Fig. 1 shows the SEM micrographs of aerobic granules before and after the adsorption of copper ions. It is readily observed that aerobic granule sludge was rugged with surface protuberances (Fig. 1(a)), but became much smoother after Cu^{2+} adsorption (Fig. 1(b)), and no obvious pores were observed on aerobic granules surface; this result agree well with the BET measurement. This predicts that thin layer of the Cu^{2+} has covered the external surface of aerobic granules. The results from the EDS quantitative microanalysis of the sample before and after the adsorption are presented in

Table 1. The major elements for aerobic granules are C (47.728 wt.%), O (34.238%), and N (11.946%) while contents in the composition of Cu are not detected. After the adsorption process, the adsorbent contains Cu (0.624%), which indicates that most Cu^{2+} were accumulated on the surface of aerobic granules. In addition, it was noticed that the Na, Mg, K, and Ca decreased from 1.757, 0.384, 0.455, and 0.548 to 0.508, 0.309, 0.308, and 0.221%, respectively. These results implied that the ion-exchange was involved in the Cu^{2+} adsorption [15,16].

3.2. Determination of pH_{ZCP} on aerobic granular sludge

The influence of the solution pH on the Cu^{2+} uptake can be explained on the basis of the zero charge point (ZCP) or isoelectric point of the biosorbent. The ZCP was determined by measuring the surface charge of product in the de-ionized water solution at various pH using zeta-potential analyzer. Fig. 2 illustrates the relationship between zeta potential and the pH of the solution. In this study, the pH_{ZCP} of aerobic granular sludge was around 2.5, indicating that aerobic granular sludge had high negative surface charge. At the $\text{pH} > \text{pH}_{\text{ZCP}}$, the surface of the biosorbent gets negatively charged thereby supporting the more Cu^{2+} uptake due to electrostatic force of attraction. At the $\text{pH} < \text{pH}_{\text{ZCP}}$, the H^+ compete effectively with Cu^{2+} on binding sites causing a decrease in q_e [17,18].

3.3. Effect of pH

The initial solution pH influences both the binding sites in the biosorbent surface and also the solution chemistry, so the pH is an important parameter that affects Cu^{2+} sorption [17]. Fig. 3 shows the effect of initial solution pH on the amount of Cu^{2+} absorbed

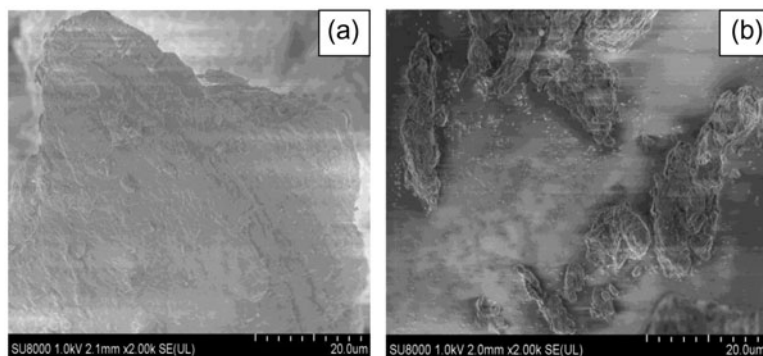


Fig. 1. SEM images of aerobic granular sludge before (a) and after (b) Cu^{2+} adsorption.

Table 1
Elemental compositions of aerobic granular sludge before and after adsorption

Element	Before adsorption		After adsorption	
	wt.%	at.%	wt.%	at.%
C	47.728	55.264	48.564	56.673
N	11.946	12.127	9.863	9.512
O	34.238	29.753	35.803	31.357
Na	1.757	1.039	0.508	0.284
Mg	0.384	0.197	0.309	0.154
Al	0.876	0.432	0.854	0.424
Si	0.243	0.102	0.835	0.399
P	1.040	0.448	1.129	0.497
S	0.431	0.173	0.686	0.286
Cl	0.354	0.128	0.296	0.106
K	0.455	0.181	0.308	0.067
Ca	0.548	0.156	0.221	0.103
Cu	–	–	0.624	0.139
Total	100.000	100.000	100.000	100.000

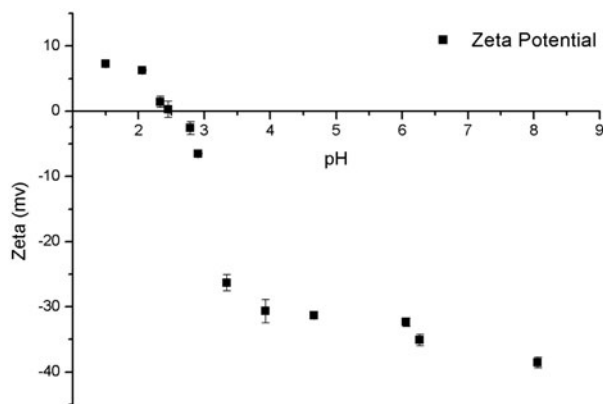


Fig. 2. pH_{zcp} curve of aerobic granular sludge.

(mg g^{-1}) at equilibrium conditions. From Fig. 3, it was observed that the amount of Cu^{2+} adsorbed increased with an increase in pH from 2.28 to 5.19. This could be explained that the lowering of pH caused the surface of the adsorbent to be protonated to a higher extent, thereby decreasing the biosorption capacity of Cu^{2+} because of competitive adsorption of protons [19,20].

Fig. 3 (inset) depicts the change of initial and terminal pH in solution. It can be observed that the value of terminal pH increased a little after adsorption when initial pH was in the range of 2–4.5, but it decreased when initial pH was higher than 4.5. According to the acid–base theory of Lewis, it can be explained that the protonation of activated site groups are most likely to occur for Cu^{2+} as a role of Lewis base under high

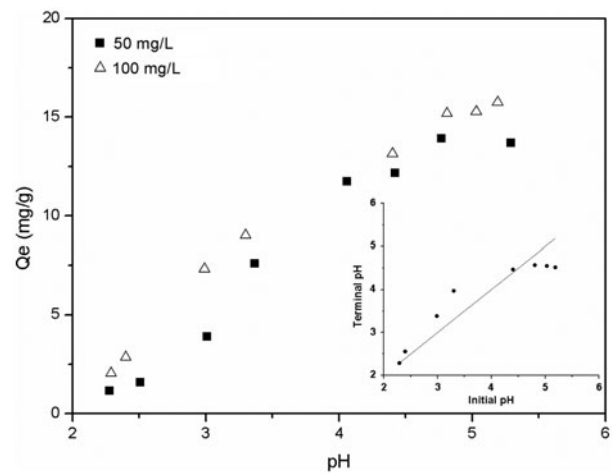


Fig. 3. Effects of pH on adsorption of Cu^{2+} .

acidic condition. In the similar way, Cu^{2+} can be a Lewis acid with the increase in the initial pH, and the deprotonation of activated site groups occurred and resulted in a release of H^+ [21]. Similar observations were also reported by Chen et al. [22].

3.4. Effect of contact time and initial Cu^{2+} concentrations

Fig. 4 shows the effect of contact time on adsorption of Cu^{2+} at different initial Cu^{2+} concentrations. As shown in Fig. 4, the adsorption capacity increased from 13.57 to 16.8 mg g^{-1} with the increase in the initial Cu^{2+} concentration from 30 to 150 mg L^{-1} at 25 °C. This may be attributed to the high initial concentration providing a significant driving force to overcome all mass transfer resistance of metal ions between the aqueous and solid phases. Besides, a two-stage behav-

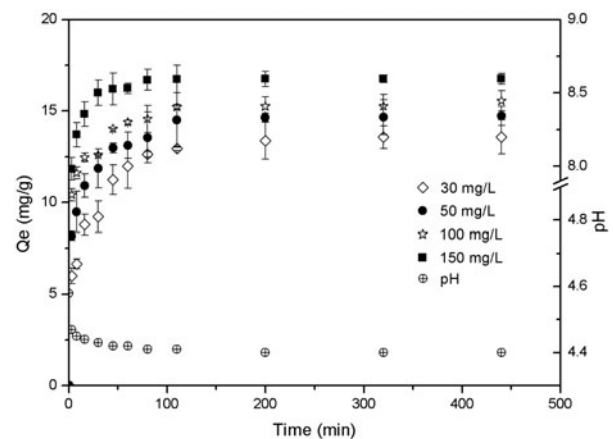


Fig. 4. Effects of time on adsorption of Cu^{2+} .

ior was observed; it could be noted that the adsorption was rapid in the initial stage and gradually decreased to equilibrium with progress of adsorption. This is probably due to the availability of active sites around or inside the surface in the first stage. In the second stage, with the gradual occupancy of active sites, the adsorption saturation could be all completely reached within 120 min [23]. In order to get the maximum uptake, the contact time was determined to be 2 h during the batch studies.

Furthermore, a rather fast uptake of Cu^{2+} and a small decrease of pH values from 4.58 to 4.42 in the fast adsorption stage was observed, which may be due to the adsorption of Cu^{2+} on the adsorbent surface functional groups such as hydroxyl, carboxyl, and amino resulting in a release of H^+ . With the saturated adsorption of active sites, the value of pH tends to be stable gradually.

3.5. Effects of biosorbent dosage

The effects of adsorbent dose on equilibrium uptake capacity, q_e (mg g^{-1}), and removal efficient (%) for the adsorbent are shown in Fig. 5. It was observed that the amount of Cu^{2+} adsorbed onto unit weight of aerobic granules decreased with the increase in the initial biomass concentration. The Cu^{2+} uptake decreased from 37.12 to 15.94 mg g^{-1} for an increase in biomass concentration from 0.1 to 1.0 g. However, the removal efficiency (%) increased from 3.7 to 16.56%, which is due to the increase in the vacant adsorption sites with increasing biomass thus favoring more Cu^{2+} uptake. The decrease in q_e may be due to the reduction in overall surface area of the biosorbent probably because of aggregation during the sorption [18,24,25].

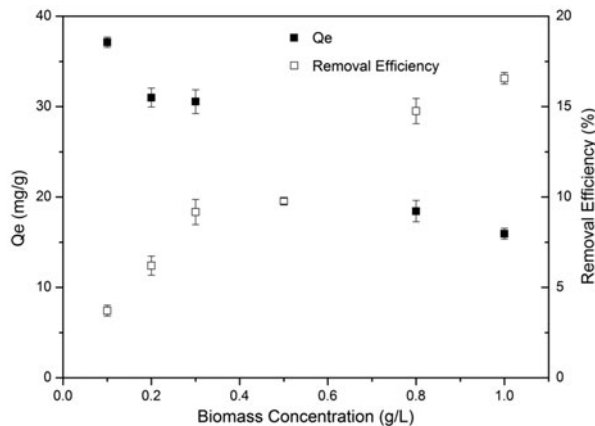


Fig. 5. Effects of biosorbent dosage on adsorption of Cu^{2+} .

3.6. Adsorption isotherms

Adsorption isotherms are important for the description of how biosorbate will interact with a biosorbent. The experimental equilibrium data in this work were fitted to the three widely used Langmuir [26], Freundlich [27], and Redlich–Peterson isotherm models [28] by non-linear method.

The Langmuir isotherm:

$$q_e = \frac{Q^0 K_L C_e}{1 + K_L C_e} \quad (1)$$

The Freundlich isotherm:

$$q_e = K_F C_e^{\frac{1}{n}} \quad (2)$$

The Redlich–Peterson isotherm:

$$q_e = \frac{A C_e}{1 + B C_e^\beta} \quad (3)$$

where q_e takes the same meaning as that in Eqs. (1)–(3), C_e the equilibrium concentration of the heavy metal ion in the solution (mg L^{-1}), Q^0 the maximum amount of metal ion uptake per unit mass of the sorbent (mg g^{-1}), and K_L the Langmuir affinity constant (L mg^{-1}). Where K_F denotes the relative adsorption capacity (mg g^{-1}) and n the intensity of adsorption. A (L g^{-1}) and B (L mmol^{-1}) $^\beta$ are the Redlich–Peterson isotherm constants, while β is the Redlich–Peterson isotherm exponent. For $\beta = 1$, the Redlich–Peterson model converts to the Langmuir model.

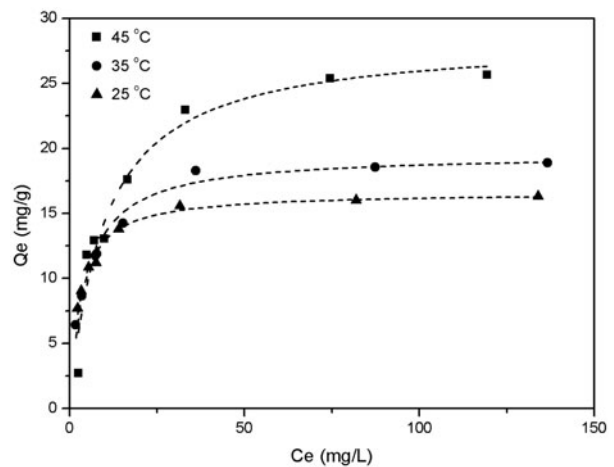


Fig. 6. Sorption isotherms of Cu^{2+} on aerobic granular sludge at different temperatures.

Sorption isotherms of Cu^{2+} on aerobic granular sludge at different temperatures (25, 35, and 45°C) are shown in Fig. 6, the best fitting curves were performed using Langmuir model. The values of parameters in Langmuir (Q^0 and K_L), Freundlich (K_F and n), and Redlich–Peterson (A , B , and β) were determined and are reported in Table 2. As can be seen from Table 2, the Langmuir isotherms and Redlich–Peterson isotherms fit better to the experimental results comparing to the Freundlich isotherm models. Besides, the value of β is pretty close to 1. It confirmed the monolayer adsorption process of Cu^{2+} onto aerobic granular sludge [29]. In addition, calculating the parameter of R_L can determine whether the adsorption process is favorable [23]. The dimensionless adsorption intensity (R_L) was calculated using the following formula:

$$R_L = \frac{1}{1 + K_L C_0} \quad (4)$$

where C_0 (mg L^{-1}) is the initial Cu^{2+} concentration and K_L the Langmuir affinity constant (L mg^{-1}). According to the value of separation factor R_L : (1) favorable adsorption $0 < R_L < 1$; (2) unfavorable adsorption $R_L > 1$; (3) linear adsorption $R_L = 1$; and (4) irreversible adsorption $R_L = 0$.

The values of R_L for $C_0 = 100 \text{ mg L}^{-1}$ were calculated to be 0.028, 0.043, and 0.089 for Cu^{2+} adsorption on aerobic granular sludge at 25, 35, and 45°C, respectively. It confirmed that the adsorption process was favorable.

3.7. Adsorption kinetics

The several kinetic models are needed to determine the data to examine the mechanism of adsorption process such as mass transfer and chemical reaction. Three sorption kinetic models were used in this work to describe the sorption characteristics.

The first model is the pseudo-first-order rate equation as expressed in Eq. (5).

$$\frac{dq}{dt} = k_1(q_e - q) \quad (5)$$

Integrating Eq. (5) from $t=0$ to $t=t$ and $q=0$ to $q=q$ results in:

$$q = q_e(1 - e^{-k_1 t}) \quad (6)$$

The second model is pseudo-second-order rate equation as expressed in Eq. (7).

$$\frac{dq}{dt} = k_2(q_e - q)^2 \quad (7)$$

Integrating Eq. (7) from $t=0$ to $t=t$ and $q=0$ to $q=q$ leads to:

$$q = \frac{q_e^2 k_2 t}{1 + q_e k_2 t} \quad (8)$$

In Eqs. (5)–(8), t is the contact time (min), q the sorption capacity of metal ion at time (mg g^{-1}), q_e the sorption capacity at equilibrium (mg g^{-1}), k_1 the first-order rate constant (min^{-1}), while k_2 the second-order rate constant ($\text{g mg}^{-1} \text{min}^{-1}$).

Weber and Morris sorption kinetic model is expressed as:

$$q = k_{\text{int}} t^{0.5} + I \quad (9)$$

where k_{int} is the Weber and Morris intraparticle diffusion rate ($\text{mg g}^{-1} \text{min}^{-0.5}$), and I the intercept of vertical axis (mg g^{-1}).

The calculated kinetic constants are shown in Table 3. The results showed that the pseudo-second-order model fitted the simulation curve much better than the pseudo-first-order model. Furthermore, the value of k_2 gets increased with increase in the initial Cu^{2+} concentration. It means that the higher the initial concentration of Cu^{2+} , the faster the adsorption rate.

Table 2

Parameters of adsorption isotherms of different temperatures for Cu^{2+} on aerobic granular sludge

T (°C)	Langmuir			Freundlich			Redlich–Peterson			
	Q^0 (mg g^{-1})	K_L (L mg^{-1})	R^2	n	K_F (mg g^{-1})	R^2	A (L g^{-1})	B (L mmol^{-1})	β	R^2
25	16.614	0.348	0.985	6.377	8.118	0.860	6.357	0.416	0.981	0.984
35	19.555	0.220	0.979	4.904	7.542	0.877	4.980	0.298	0.965	0.978
45	28.478	0.102	0.949	3.303	6.688	0.828	2.548	0.065	1.069	0.942

Table 3

Parameters of adsorption kinetics of different initial concentrations for Cu²⁺ on aerobic granular sludge

Initial concentration (mg L ⁻¹)	Pseudo-first order			Pseudo-second order		
	$q_{e,1}$ (mg g ⁻¹)	k_1 (min ⁻¹)	R^2	$q_{e,2}$ (mg g ⁻¹)	k_2 (g mg ⁻¹ min ⁻¹)	R^2
30	12.570	0.085	0.880	13.492	0.010	0.953
50	13.508	0.198	0.897	14.284	0.021	0.967
100	14.237	0.369	0.919	14.855	0.039	0.968
150	16.205	0.385	0.970	16.741	0.042	0.996
Initial concentration (mg L ⁻¹)	Weber–Morris					
	I (mg g ⁻¹)	K_{int} (mg g ⁻¹ min ^{-0.5})	RC (%)	R^2		
30	2.846	1.123	21.094	0.868		
50	4.075	1.267	28.528	0.735		
100	4.772	1.476	32.124	0.621		
150	3.615	2.727	21.594	0.703		

Generally, the sorption includes three steps as follows: (1) sorbate transfers from the boundary film to surface of sorbent (external mass transfer step), (2) sorbate transfers from the sorbent surface to intraparticle active site or binding site (intraparticle diffusion step), and (3) sorption of the sorbate on the active or binding sites of sorbent [18]. In order to further investigate the adsorption of intraparticle diffusion coefficient, Weber–Morris model are used in this study. It was observed that the values of initial adsorption rates k_{int} increased with an increase in the initial Cu²⁺ concentration; results indicated that the intraparticle diffusion rate increased with the increase in initial Cu²⁺ concentration. This could be attributed to the increase in the driving force for the mass transfer. Furthermore, calculating the value of relative coefficient (RC) can determine whether the external mass transfer and intraparticle diffusion were considered as rate-limiting step [30]. The RC which is expressed as the ratio between the intercept (I) and the equilibrium sorption capacity is as follows:

$$RC (\%) = 100 \frac{I}{q_e} \quad (10)$$

where I takes the same meaning as Eq. (9), and q_e the equilibrium sorption capacity was obtained from the best fitted kinetic model. The higher RC would indicate that the external mass transfer step was a rate-limiting step, whereas the lower RC indicated that the intraparticle diffusion step was the rate-limiting

step. In this work, q_e from the pseudo-second-order kinetic model was applied in Eq. (8) and the values of RC are reported in Table 3. It can be seen from the table that RC took the values only between about 21–32% (RC lower than 50%), which indicated that the intraparticle diffusion was more significant as a rate-limiting step than the external mass transfer. Moreover, according to the equilibrium adsorption capacity (16.614 mg g⁻¹) of Cu²⁺ on aerobic granules at 25°C, the weight percentage of Cu on adsorbent should be 1.661%. However, from the results of EDS surface elemental analysis of Cu in Table 1, it only gives 0.624 wt.%, which is much lower; although the element analysis of EDS is not accurate due to the selection of different sampling positions, qualitative analysis can be acceptable as the metal ions accumulate on the surface of the adsorbent. Thus, this may imply that the intraparticle diffusion occurred and appeared more significant although the pore size in aerobic granules not appeared much remarkable, and it is in accordance with the results from kinetics process.

3.8. Adsorption thermodynamic

Thermodynamic parameters of sorption of Cu²⁺ onto aerobic granules were evaluated using the following equations:

$$\Delta G^0 = -RT \cdot \ln Kc \quad (11)$$

$$\ln Kc = -\Delta H^0/RT + \text{const} \quad (12)$$

$$\Delta G^0 = \Delta H^0 - T\Delta S^0 \quad (13)$$

where ΔH^0 , ΔS^0 , ΔG^0 , and T are the enthalpy (kJ mol^{-1}), entropy ($\text{kJ mol}^{-1} \text{K}^{-1}$), Gibbs free energy (kJ mol^{-1}), and absolute temperature (K), respectively; R is the gas constant ($8.13 \text{ J mol}^{-1} \text{K}^{-1}$) and Kc is the equilibrium constant (L mol^{-1}).

The thermodynamic parameters are listed in Table 4. The negative value of ΔG^0 indicated the spontaneous nature of adsorption process. Positive value of ΔH^0 indicated the endothermic enthalpy of adsorption favored by increased temperature. This effect may be due to the fact that at a higher temperature, an increase in active sites occurs owing to bond rupture of functional groups on adsorbent surface [31]. While the positive value of ΔS^0 shows the affinity of the adsorption for Cu^{2+} [32].

3.9. Adsorption mechanisms

3.9.1. FTIR Analysis

FTIR spectra of aerobic granular sludge were recorded to obtain information on the chemical function groups of the adsorbent surface. The FTIR spectra before and after adsorption of aerobic granular sludge are shown in Fig. 7.

In Fig. 7(a), the broad and strong band at $3,408.18 \text{ cm}^{-1}$ may be due to the overlapping of O–H and N–H stretching. The peak at $2,929.72$ and $2,853.17 \text{ cm}^{-1}$ exhibited the C–H stretching vibrations of –CH. At $1,731.36 \text{ cm}^{-1}$, it was a characteristic peak of stretching vibration of C=O. The band at $1,650.77 \text{ cm}^{-1}$ was the result of the stretching vibration of N–H (Amide I) and C=O. A distinct band at $1,454.59 \text{ cm}^{-1}$ could be due to bending vibration of –CH₂. While the band at $1,548.56 \text{ cm}^{-1}$ could be assigned to a combination of the stretching vibration of C–N and deformation vibration of N–H peptide bond of protein (Amide II). The band

Table 4

Parameters of adsorption thermodynamic of different temperatures for Cu^{2+} on aerobic granular sludge

T ($^{\circ}\text{C}$)	ΔG^0 (kJ mol^{-1})	ΔH^{0a} (kJ mol^{-1})	$T\Delta S^0$ (kJ mol^{-1})
25	–1.504	25.305	26.809
35	–1.535		26.840
45	–2.632		27.937

^aMeasured between 25 and 45°C .

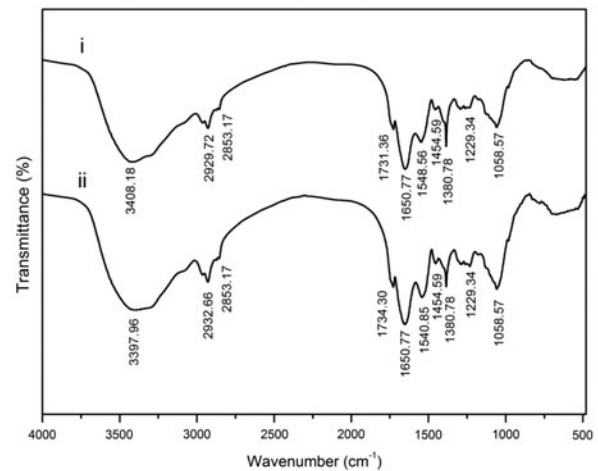


Fig. 7. The FTIR spectra of aerobic granular sludge before (a) and after (b) adsorption.

at $1,229.34 \text{ cm}^{-1}$ could be attributed to the C–N stretching of Amide III. Band at $1,058.57 \text{ cm}^{-1}$ was the result of stretching vibration of C–O. And the finger region demonstrated the existence of sulfur or phosphate groups [33]. The FTIR analysis of aerobic granular sludge proved that there were most active functional groups such as hydroxyl, carboxyl, and amino groups existed on the surface of sludge, and which are the composition of EPS.

In Fig. 7(b), after adsorption of Cu^{2+} on 1 g L^{-1} of aerobic granular sludge at pH 4.77 and 25°C with 100 mg L^{-1} of Cu^{2+} solution, the peak shifts from $1,548.56$ to $1,540.85 \text{ cm}^{-1}$, demonstrating that a large number of hydroxyl and amine groups were introduced on the surface of aerobic granules. In addition, observed bands at $1,731.36 \text{ cm}^{-1}$ were shifted, this may be attrib-

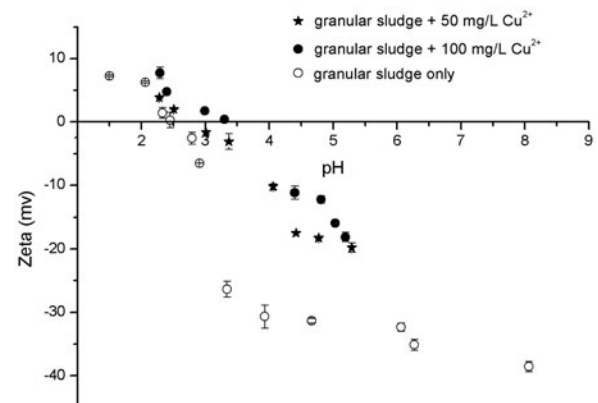


Fig. 8. pH dependence of zeta potential of aerobic granular sludge for different initial concentrations of Cu^{2+} .

uted to carboxyl groups on the aerobic granules interact with Cu^{2+} , and the results correspond with the phenomenon in the change of pH during the adsorption.

3.9.2. Zeta potential measurement

Zeta potential analysis can indirectly discriminate between inner- and outer-sphere surface complexes on aerobic granular sludge [34]. Fig. 8 presents data on the pH dependency of zeta potentials for different initial Cu^{2+} concentrations.

Over the full pH range studied, there are much negative charges existed on the surface of aerobic granular sludge with very low pH_{ZCP} values. And this would facilitate the adsorption of Cu^{2+} due to electrostatic force of attraction. After Cu^{2+} loading, the zeta potential values of aerobic granules shifted positively. The positive shift in surface charge suggested that Cu^{2+} was adsorbed as cationic or neutral inner-sphere surface complexes that could make the net surface charge less negative [35,36]. Fig. 8 shows that an increase of initial Cu^{2+} concentration shifted the pH_{ZCP} of aerobic granular sludge toward higher and higher pH values. This is probably because q_e increased with the increase in the concentration of Cu^{2+} , as a result, the pH_{ZCP} was shifted positively more.

4. Conclusions

The adsorption of Cu^{2+} on aerobic granular sludge was studied. The pH_{ZCP} of aerobic granular sludge was measured at around 2.5. The initial solution pH had a strong influence on Cu^{2+} sorption, q_e increased with the increase in pH values. On the contrary, it decreased with increase in the biomass concentration. The effect of contact time showed that the absorption equilibrium could be achieved only after 120 min. The adsorption isotherms data were fitted by Langmuir isotherms, predicting the adsorption of Cu^{2+} on aerobic granules was a monolayer adsorption, and the values of R_L confirmed that the adsorption process is favorable. The adsorption kinetics data were well described by a pseudo-second-order kinetic model. The sorption of Cu^{2+} was controlled primarily by intraparticle diffusion combined with the kinetics process with EDS analysis. Parameters of adsorption thermodynamic suggested that the interaction of Cu^{2+} adsorbed by aerobic granules was spontaneous and endothermic. According to variations in EDS and FTIR results before and after adsorption, it is considered that ion-exchange and surface complexation mecha-

nism coexisted. Moreover, zeta potential analysis also demonstrated inner-sphere adsorption happened for Cu^{2+} adsorption on aerobic granules.

Acknowledgments

The work was supported by project No. 2009AE01601 and project No. 20132BAB203033 from Jiangxi Science and Technology Bureau.

References

- [1] H. Kozłowski, A. Janicka Klos, J. Brasun, E. Gaggelli, D. Valensin, G. Valensin, Copper, iron, and zinc ions homeostasis and their role in neurodegenerative disorders (metal uptake, transport, distribution and regulation), *Coord. Chem. Rev.* 253 (2009) 2665–2685.
- [2] F. Fu, Q. Wang, Removal of heavy metal ions from wastewaters: A review, *J. Environ. Manage.* 92 (2011) 407–418.
- [3] B.W. Atkinson, F. Bux, H.C. Kusan, Considerations for application of biosorption technology to remediate metal-contaminated industrial effluents, *Water SA* 24 (1998) 129–135.
- [4] B. Volesky, Biosorption and me, *Water Res.* 41 (2007) 4017–4029.
- [5] S.O. Lesmana, N. Febriana, F.E. Soetaredjo, J. Sunarso, S. Ismadji, Studies on potential applications of biomass for the separation of heavy metals from water and wastewater, *Biochem. Eng. J.* 44 (2009) 19–41.
- [6] J.L. Wang, C. Chen, Biosorption of heavy metals by *Saccharomyces cerevisiae*: A review, *Biotechnol. Adv.* 24 (2006) 427–451.
- [7] D. Sud, G. Mahajan, M.P. Kaur, Agricultural waste material as potential adsorbent for sequestering heavy metal ions from aqueous solutions—A review, *Bioresour. Technol.* 99 (2008) 6017–6027.
- [8] M. Šćiban, B. Radetić, Ž. Kevrešan, M. Klačnja, Adsorption of heavy metals from electroplating wastewater by wood sawdust, *Bioresour. Technol.* 98 (2007) 402–409.
- [9] X. Han, Y.S. Wong, M.H. Wong, N.F.Y. Tam, Biosorption and bioreduction of Cr(VI) by a microalgal isolate, *Chlorella miniata*, *J. Hazard. Mater.* 146 (2007) 65–72.
- [10] J.Y. Farah, N.S. El-Gendy, L.A. Farahat, Biosorption of Astrazone Blue basic dye from an aqueous solution using dried biomass of Baker's yeast, *J. Hazard. Mater.* 148 (2007) 402–408.
- [11] S.S. Ahluwalia, D. Goyal, Microbial and plant derived biomass for removal of heavy metals from wastewater, *Bioresour. Technol.* 98 (2007) 2243–2257.
- [12] Y. Liu, S.F. Yang, S.F. Tan, Y.M. Lin, J.H. Tay, Aerobic granules: A novel zinc biosorbent, *Lett. Appl. Microbiol.* 35 (2002) 548–551.
- [13] Y. Liu, H. Xu, S.F. Yang, J.H. Tay, A general model for biosorption of Cd^{2+} , Cu^{2+} and Zn^{2+} by aerobic granules, *J. Biotechnol.* 102 (2003) 233–239.
- [14] H. Xu, Y. Liu, J.H. Tay, Effect of pH on nickel biosorption by aerobic granular sludge, *Bioresour. Technol.* 97 (2006) 359–363.

- [15] X.H. Wang, R.H. Song, S.X. Teng, M.M. Gao, J.Y. Ni, F.F. Liu, S.G. Wang, B.Y. Gao, Characteristics and mechanisms of Cu(II) biosorption by disintegrated aerobic granules, *J. Hazard. Mater.* 179 (2010) 431–437.
- [16] H. Chen, G.L. Dai, J. Zhao, A.G. Zhong, J.Y. Wu, H. Yan, Removal of copper(II) ions by a biosorbent—*Cinnamomum camphora* leaves powder, *J. Hazard. Mater.* 177 (2010) 228–236.
- [17] X.F. Sun, S.G. Wang, X.W. Liu, W.X. Gong, N. Bao, Y. Ma, The effects of pH and ionic strength on fulvic acid uptake by chitosan hydrogel beads, *Colloids Surf. A* 324 (2008) 28–34.
- [18] K.V. Kumar, K. Porkodi, Mass transfer, kinetics and equilibrium studies for the biosorption of methylene blue using *Paspalum notatum*, *J. Hazard. Mater.* 146 (2007) 214–226.
- [19] L.H. Gai, S.G. Wang, W.X. Gong, X.W. Liu, B.Y. Gao, H.Y. Zhang, Influence of pH and ionic strength on Cu (II) biosorption by aerobic granular sludge and biosorption mechanism, *J. Chem. Technol. Biotechnol.* 83 (2008) 806–813.
- [20] S.G. Wang, X.F. Sun, X.W. Liu, W.X. Gong, B.Y. Gao, N. Bao, Chitosan hydrogel beads for fulvic acid adsorption: Behaviors and mechanisms, *Chem. Eng. J.* 142 (2008) 239–247.
- [21] W. Stumm, L. Sigg, J.L. Schnoor, Aquatic chemistry of acid deposition, *Environ. Sci. Technol.* 21 (1987) 8–13.
- [22] Z. Chen, W. Ma, M. Han, Biosorption of nickel and copper onto treated alga *Undaria pinnatifida*: Application of isotherm and kinetic models, *J. Hazard. Mater.* 155 (2008) 327–333.
- [23] N. Ertugay, Y.K. Bayhan, Biosorption of Cr (VI) from aqueous solutions by biomass of *Agaricus bisporus*, *J. Hazard. Mater.* 154 (2008) 432–439.
- [24] Z. Wang, D.E. Giammar, Mass action expressions for bidentate adsorption in surface complexation modeling: Theory and practice, *Environ. Sci. Technol.* 47 (2013) 3982–3996.
- [25] D.M. Di Toro, J.D. Mahony, P.R. Kirchgraber, A.L. O'Byrne, L.R. Pasquale, D.C. Piccirilli, Effects of nonreversibility, particle concentration, and ionic strength on heavy-metal sorption, *Environ. Sci. Technol.* 20 (1986) 55–61.
- [26] I. Langmuir, The constitution and fundamental properties of solids and liquids. Part I. Solids, *J. Am. Chem. Soc.* 38 (1916) 2221–2295.
- [27] H. Freundlich, Over the adsorption in solution, *J. Phys. Chem.* 57 (1906) 385–470.
- [28] O. Redlich, D.L. Peterson, A useful adsorption isotherm, *J. Phys. Chem.* 63 (1959) 1024–1024.
- [29] V.K. Gupta, A. Rastogi, A. Nayak, Adsorption studies on the removal of hexavalent chromium from aqueous solution using a low cost fertilizer industry waste material, *J. Colloid Interface Sci.* 342 (2010) 135–141.
- [30] R. Apiratikul, P. Pavasant, Sorption of Cu²⁺, Cd²⁺, and Pb²⁺ using modified zeolite from coal fly ash, *Chem. Eng. J.* 144 (2008) 245–258.
- [31] Z. Aksu, Determination of the equilibrium, kinetic and thermodynamic parameters of the batch biosorption of nickel(II) ions onto *Chlorella vulgaris*, *Process Biochem.* 38 (2002) 89–99.
- [32] X.F. Sun, S.G. Wang, X.W. Liu, W.X. Gong, N. Bao, B.Y. Gao, H.Y. Zhang, Biosorption of Malachite Green from aqueous solutions onto aerobic granules: Kinetic and equilibrium studies, *Bioresour. Technol.* 99 (2008) 3475–3483.
- [33] J.F. Gao, Q. Zhang, J.H. Wang, X.L. Wu, S.Y. Wang, Y.Z. Peng, Contributions of functional groups and extracellular polymeric substances on the biosorption of dyes by aerobic granules, *Bioresour. Technol.* 102 (2011) 805–813.
- [34] W. Stumm, J.J. Morgan, *Aquatic Chemistry*, 3rd ed., Wiley Interscience, New York, NY, 1996.
- [35] M. Del Nero, C. Galindo, R. Barillon, E. Halter, B. Madé, Surface reactivity of α -Al₂O₃ and mechanisms of phosphate sorption: *In situ* ATR-FTIR spectroscopy and ζ potential studies, *J. Colloid Interface Sci.* 342 (2010) 437–444.
- [36] Z. Wang, S.W. Lee, J.G. Catalano, J.S. Lezama-Pacheco, J.R. Bargar, B.M. Tebo, D.E. Giammar, Adsorption of uranium(VI) to manganese oxides: X-ray absorption spectroscopy and surface complexation modeling, *Environ. Sci. Technol.* 47 (2013) 850–858.